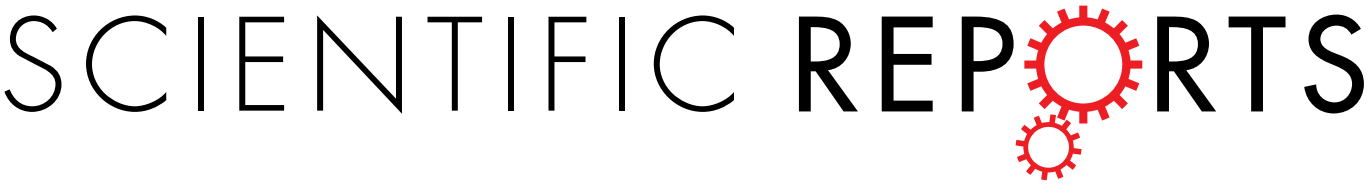

OPEN

Phosphorus K_4 Crystal: A New Stable Allotrope

Jie Liu[1,2,3], Shunhong Zhang[1,2], Yaguang Guo[1,2] & Qian Wang[1,2,3]

Received: 12 May 2016
Accepted: 26 October 2016
Published: 18 November 2016

The intriguing properties of phosphorene motivate scientists to further explore the structures and properties of phosphorus materials. Here, we report a new allotrope named K_4 phosphorus composed of three-coordinated phosphorus atoms in non-layered structure which is not only dynamically and mechanically stable, but also possesses thermal stability comparable to that of the orthorhombic black phosphorus (*A*17). Due to its unique configuration, K_4 phosphorus exhibits exceptional properties: it possesses a band gap of 1.54 eV which is much larger than that of black phosphorus (0.30 eV), and it is stiffer than black phosphorus. The band gap of the newly predicted phase can be effectively tuned by appling hydrostastic pressure. In addition, K_4 phosphorus exibits a good light absorption in visible and near ultraviolet region. These findings add additional features to the phosphorus family with new potential applications in nanoelectronics and nanomechanics.

Phosphorus is a common material for industrialized production of fertilizers, organophosphorus compounds, matches, and so on. Because of its high chemical reactivity and strong toxicity, this material has received little academic attention until recently[1]. In 2014 phosphorus was brought to spotlight by successfully fabricating the field-effect transistors (FETs) constructed using the exfoliated black phosphorus and finding their outstanding performance by two independent groups[2,3], which was exactly 100 years after the discovery of black phosphorus[4]. Recently, monolayer black phosphorus (phosphorene), as a new member of two dimensional (2D) materials family, has attracted tremendous attention to explore the structural varieties[5], electronic properties[6], unique mechanical features[7], and promising applications in electronics[8] and gas sensors[9].

Like carbon and boron, phosphorus displays fascinating structural variability. The stable allotropes of phosphorus at ambient conditions can be classified into three major categories: white phosphorus[10], orthorhombic black phosphorus[4], and various forms of red phosphorus[11]. White phosphorus is highly reactive with air and forms three crystal structures including α-, β-, and γ-P_4[12]. Black phosphorus possesses an orthorhombic structure (*A*17, space group: *Cmca*) at ambient conditions and transforms to rhombohedral structure (*A*7, space group: $R\bar{3}m$) at around 5 GPa[12]. While the *A*7 structure transforms to an α-Po-type simple cubic three dimensional (3D) structure (space group: *Pm3m*) at a higher pressure of about 10 GPa[10]. Amorphous and crystalline forms of red phosphorus can be evolved from white phosphorus by heating it to higher than 20 °C[13]. The various forms of red phosphorus are based on tubular units of five- and six-membered rings[12]. Although a number of the allotropes of phosphorus have already been experimentally characterized or theoretically predicted[4,12,14] the discovery of new phases of phosphorus has attracted continued attention[15,16]. Since the most stable phase of phosphorus is the three-coordinated *layered* black phosphorus, an interesting question then raises: can we find a stable 3D *non-layered* allotrope of phosphorus at ambient conditions which is also composed of only three-coordinated atoms?

Inspired by the unique geometry of K_4 structure where the coordination number of each atom is three, we explore the stability and properties of phosphorus in K_4 crystal structure. In fact, since the identification of K_4 geometry in mathematics in 2008[17], design and synthesis of pristine elemental substances in K_4 structure have been an attractive scientific topic. The nitrogen K_4 crystal named cg-N (cubic gauche) was synthesized from molecular nitrogen under pressure above 110 GPa using a laser-heated diamond cell[18]. The coordination polymers and metal-organic frameworks having the topology of K_4 crystal were reported in 1990s[19]. A K_4 crystal carbon was proposed to be a possible metallic allotrope of carbon in 2009[20]. Unfortunately, a latter work suggested that K_4 carbon is dynamically unstable[21]. In 2010, Dai *et al.* proposed a boron K_4 crystal that is stable under

[1]Center for Applied Physics and Technology, College of Engineering, Peking University; Key Laboratory of High Energy Density Physics Simulation, Ministry of Education, Beijing 100871, China. [2]Department of Materials Science and Engineering, College of Engineering, Peking University, Beijing 100871, China. [3]Collaborative Innovation Center of IFSA (CICIFSA), Shanghai Jiao Tong University, Shanghai 200240, China. Correspondence and requests for materials should be addressed to Q.W. (email: qianwang2@pku.edu.cn)

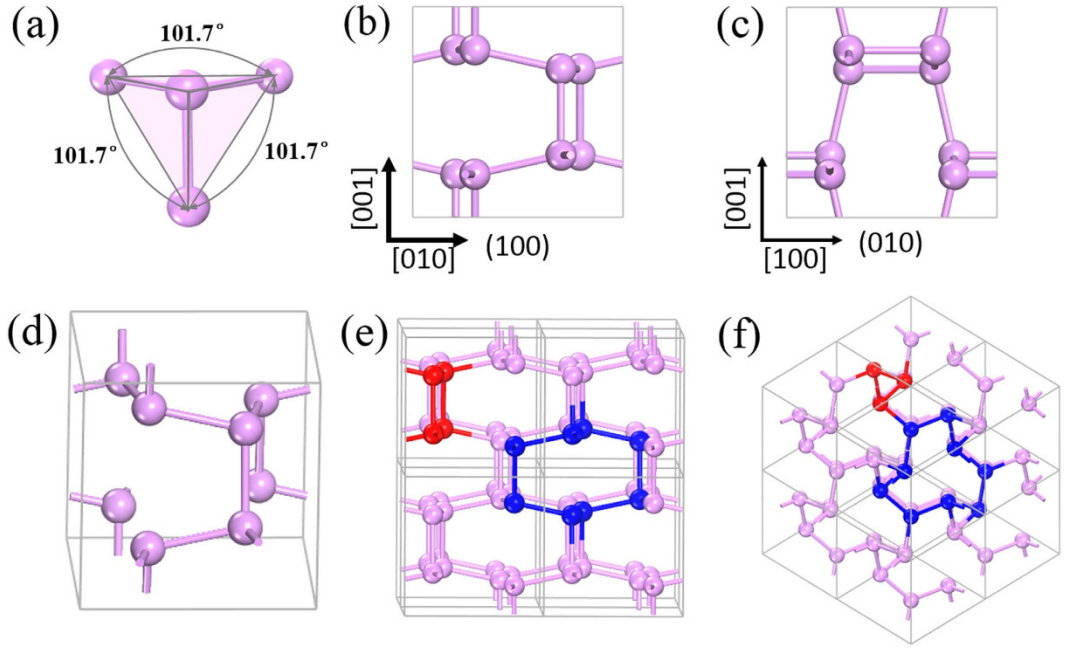

Figure 1. Optimized crystal structure of K_4 phosphorus. (**a**) Building block of K_4 phosphorus. (**b**)–(**c**) Crystal structure of K_4 phosphorus viewed from the [100] and [010] directions. (**d**) Perspective view of the conventional unit cell of K_4 phosphorus. (**e**) and (**f**) Two different perspective views of a $2 \times 2 \times 2$ supercell to display the charity.

	a	*b*	*c*	V_0	ΔE	E_g
K_4	5.37[a]	5.37	5.37	19.36[a]	0.02[a]	1.13[a]
	5.32[b]	5.32	5.32	18.82[a]	0.04[b]	1.54[d] (1.07[b])
*A*17	3.28[a]	11.22[a]	4.54[a]	20.89[a]	—	—
	3.32[b]	10.43[b]	4.41[b]	19.09[a]	—	0.36[d] (0.08[a])
	3.3133[c]	10.473[c]	4.374[c]	18.97[a]	—	0.335[c]

Table 1. Calculated lattice parameters (*a*, *b*, and *c* in Å), volume (V_0 in Å^3/atom), relative energies with respect to that of black phosphorus (ΔE in eV/atom), and energy band gaps (E_g in eV). [a]Our calculated results at the PBE level. [b]Our calculated results at the GGA-D2 level. [c]Experimental data[12]. [d]Our calculated results at the HES06 level.

ambient pressure[22]. All these progresses, especially experimental realization of high pressure polymeric nitrogen in K_4 structure, make the exploration of K_4 phosphorus structure very promising.

In this work, the dynamical, thermal, and mechanical stabilities of K_4 phosphorus structure are confirmed, and its electronic, mechanical, and optical properties are studied based on a series of state-of-the-art calculations. The phonon vibrational modes at the first Brillouin zone center are also simulated to aid future experimental identification of the new phase of phosphorus from Raman and infrared (IR) spectroscopy.

Results and Discussion

Phosphorus K_4 structure. Different from boron K_4 crystal, where each boron atom is sp^2-hybridized, for the stable phosphorus allotropes at ambient conditions, due to the electron lone pair, each phosphorus atom is actually sp^3-hybridized which displays a tetrahedral bonding character[6]. To remain this bonding character, we conceive the idea of building a phosphorus K_4 structure using a building block composed of four phosphorus atoms in a tetrahedron configuration that is displayed in Fig. 1(a). In the building block, the central phosphorus atom is sp^3-hybridized, and connects its three neighboring atoms, thus remaining the tetrahedral bonding character of phosphorus at ambient conditions. With equal bond lengths and bond angles, this structural unit is used to build the high symmetric K_4 crystal.

As shown in Fig. 1(c) and (d), the optimized structure of phosphorus K_4 is body-centered cubic with 8 atoms located at the 8a (0.206, 0.206, 0.206) Wyckoff position in the conventional unit cell. Compared to K_4 boron, K_4 phosphorus has a reduced symmetry with the space group symmetry of T5 ($I2_13$, No. 199). The lattice parameters are optimized using both PBE and GGA-D2 functionals, and the results are presented in Table 1. The lattice parameters of black phosphorus are also calculated using the same level of theory and compared with the experimental data. We can see that K_4 phosphorus is slightly denser than the layered phosphorus structure of *A*17.

	srs	acs-g	bcu-f	eta	etd	etf	pbg
ΔE^a	0.000	0.085	0.216	0.241	0.141	0.235	0.116
ΔE^b	0.000	0.145	0.273	0.239	0.197	0.254	0.132
	pbp	**pcu-g**	**pcu-h**	**ths**	**rhr-a**	**uct**	**uto**
ΔE^a	0.608	0.563	0.023	0.017	0.409	0.308	0.293
ΔE^b	0.721	0.663	0.031	0.096	0.517	0.365	0.354

Table 2. Relative energies of hypothetical phosphorus structures with respect to the cohesive energy of K_4 phosphorus (ΔE in eV/atom). [a]Calculated results at the PBE level. [b]Calculated results at the GGA-D2 level.

However, the mass density difference is much smaller than that between diamond and graphite. This is because the electron-rich nature and the resultant Coulomb repulsion hinder phosphorus to form ultra-dense phases like diamond. As compared to black phosphorus, K_4 phosphorus has a higher symmetry, leading to an isotropic network. In the unit cell of K_4 phosphorus, only one kind of P-P bond exists and all bond angles are equivalent with a bond length of 2.24 Å/2.25 Å and a bond angle of 101.7°/102.2° at the GGA-D2/PBE level. In addition, as shown in Fig. 1(e) and (f), the three-coordinated phosphorous network displays an intriguing chirality that can be seen from the spiral square-octagon and triangle-nonagon polygons pairs.

Energetic stability. To investigate the energetic stability of K_4 phosphorus, total energy calculations are performed by using both the PBE and GGA-D2 functionals, respectively. For comparison, calculations are also carried out for black phosphorus. The results are listed in Table 1. The cohesive energy of K_4 phosphorus is found to be higher than that of black phosphorus by 0.02/0.04 eV/atom at the PBE/GGA-D2 functional, showing that K_4 phosphorus is thermodynamically metastable as compared to the most stable form of phosphorous allotropes, black phosphorus[12]. To further compare the relative stability of K_4 phosphorus with other phosphorus allotropes, the total energies of some other allotropes are also calculated at PBE/GGA-D2 level, and found that K_4 phosphorus is 0.07/0.01 eV/atom lower in energy than the simple cubic structure, and 0.08/0.14 eV/atom lower in energy than the two structures of white phosphorus (β-P_4, γ-P_4)[13], indicating that the K_4 phosphorus phase is energetically more stable than these well-known structures. To understand the reason why K_4 phosphorus is relatively stable, we investigated its atomic configuration. We note that in the three-coordinated phosphorus K_4 structure each bond angle is 101.7°, as shown in Fig. 1(a), close to that of 101.6° in the P_4H_6 molecule that was found to be the most energetically favorable configuration among those of the three-coordinated phosphorus atoms[5]. Therefore, the favorable geometry results in a good energetic stability of the K_4 structure.

To search for 3D *non-layered* phosphorus allotropes with good energetic stability at ambient conditions, we have screened many possible 3-coordintated networks. Since the phosphorus K_4 structure has the **srs** topology, by using the network topology approach based on the RCSR database[23,24], many candidate structures for 3D *non-layered* phosphorus with different network topologies can be obtained. Due to the limited computational resources, we only consider the so called uninodal (with only one type of vertex) structures. Actually there are 78 uninodal 3-coordinated nets in the RCSR database. Among them, there are 47 nets with too short non-bonded distance, and there are 1 net with the bond angles seriously deviated from that of P_4H_6 molecule (101.6°)[5]. So these 48 nets should be excluded. However, not all the 30 rest nets are suitable for forming 3D *non-layered* phosphorus structures. For example, the optimized structures of **etb** and **utp** configurations become 5-coordinated, and the optimized structure of **utg** configuration turns into phosphorus chains. Finally, only 14 nets including the **srs** net (K_4 phosphorus) are found to be the suitable candidate structures for 3D *non-layered* phosphorus allotropes in which every phosphorus atom retains the sp^3 hybridization character of tetra-phosphorus. The cohesive energy of these hypothetical phosphorus structures are calculated by using the PBE and GGA-D2 functionals, respectively. As listed in Table 2, we find that K_4 phosphorus is energetically most stable among the studied configurations.

Dynamic stability. To examine the dynamic stability of K_4 phosphorus, the lattice dynamics is studied by calculating its phonon dispersion using linear response method within density functional perturbation theory[25], where the force-constant matrix is calculated through differentiation of the Hellmann-Feynman forces on atoms with respect to the ionic coordinates. As shown in Fig. 2(a), the absence of imaginary modes in the whole Brillouin zone confirms that K_4 phosphorus is dynamically stable. The primitive cell of K_4 phosphorus contains four atoms, leading to nine optical and three acoustic branches. The optical branches can be classified into two groups with a frequency gap between them. The low energy group consisting of three optical branches is predominantly bond-bending type in character, while the high energy group consisting of six optical branches is bond-stretching type. All the three acoustic branches of K_4 phosphorus are linearly dispersed near the Γ point in different directions, confirming the relatively strong covalent bonds between the phosphorus atoms along these directions, while in the structure of black phosphorus the dispersion relation of the TA_z modes near the Γ point in the [100] and [010] directions[26] is almost in quadratic form that is contributed by the weak interlayer interactions.

Thermal stability. The thermal stability of K_4 phosphorus is examined by performing *ab initio* molecular dynamics (AIMD) simulations at 300 K with a large supercell ($3 \times 3 \times 3$). We find that no structure reconstruction occurs after heating for 8 *ps* with a time step of 1 *fs*, and the total potential energy remains almost constant during the simulation. These results suggest that the new structure is thermally stable at room temperature. The heat bath is then further elevated to 1000 K. As shown in the snapshot of atomic configuration of K_4 phosphorus at the

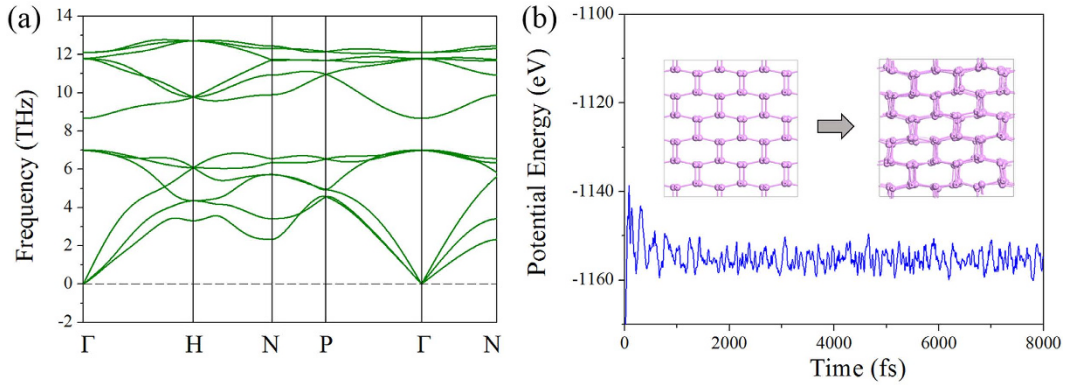

Figure 2. Structure stability of K_4 phosphorus. (**a**) Vibrational band structure of K_4 phosphorus. (**b**) Total potential energy fluctuation of K_4 phosphorus during AIMD simulation at 1000 K. The inset shows the atomic configurations ($3 \times 3 \times 3$ supercell) at the beginning and end of AIMD simulations at 1000 K.

	C_{11}	C_{22}	C_{33}	C_{44}	C_{55}	C_{66}	C_{12}	C_{13}	C_{23}	B
K_4	223.6[a]	—	—	34.6[a]	—	—	82.4[a]	—	—	129.5[a]
	232.2[b]	—	—	31.7[b]	—	—	39.3[b]	—	—	103.6[b]
*A*17	43.8[a]	188.4[a]	16.0[a]	9.8[a]	2.9[a]	58.5[a]	34.5[a]	−1.6[a]	−4.6[a]	10.9[a]
	62.8[b]	199.8[b]	83.2[b]	29.8[b]	9.6[b]	80.6[b]	43.8[b]	1.6[b]	9.3[b]	36.2[b]

Table 3. Calculated elastic constants (C_{ij} in GPa) and bulk moduli (B in GPa) of K_4 phosphorus and orthorhombic black phosphorus (*A*17). [a]Our calculated results at the PBE level. [b]Our calculated results at the GGA-D2 level.

end of AIMD simulations at 1000 K (see Fig. 2(b)), after heating for 8 *ps*, no obvious distortion in the structure appears, and the fluctuation in total potential energy still remains almost unchanged. This implies that K_4 phosphorus can withstand temperatures up to 1000 K, and this phosphorus phase is separated by high energy barriers from other local minima on the potential energy surface (PES) of elemental phosphorus.

However, it is worthy to note that the temperature for evaluating the thermal stability of a crystal structure may be overestimated by AIMD simulations due to using Canonical ensemble (NVT) during the simulations. To further investigate the thermal stability of K_4 phosphorus, the AIMD simulations are also carried out for the experimentally synthesized *A*17 structure for comparison. As shown in Fig. S1, the A17 structure can withstand the high temperature of 1000 K without any obvious structural reconstruction. However, when temperature of the heat bath is further increased to 1200 K, both the geometries of the K_4 and *A*17 phases are destroyed. The results reveal that K_4 phosphorus is thermally as stable as the *A*17 phase.

Mechanical stability and properties. To guarantee the positive definiteness of strain energy upon lattice distortion, the mechanical stability of K_4 phosphorus is examined. In the linear elastic range the elastic constant tensor forms a 6×6 matrix with 21 independent components. For a simple cubic lattice, only C_{11}, C_{12} and C_{44} are independent. The linear elastic constants of a mechanically stable 3D cubic lattice have to obey the Born-Huang criteria: $C_{11} > 0$, $C_{44} > 0$, $C_{11} > |C_{12}|$, and $(C_{11} + 2C_{12}) > 0$[27]. The elastic constants of the phosphorus K_4 crystal are derived from the strain-stress relationship by using the finite distortion method[28] implemented in VASP. All the elastic constants calculated with both the PBE and the vdW-corrected GGA-D2 functionals are listed in Table 3. These constants obey all of the Born-Huang criteria for simple cubic lattices, implying that the new structure is mechanically stable. For comparison, the calculations are also performed for *A*17, and the results are given in Table 3 as well.

The C_{11}, C_{22}, and C_{33} ($C_{11} = C_{22} = C_{33}$) elastic constants of K_4 phosphorus directly relate to sound propagation along the crystallographic *a*, *b*, and *c* axes, respectively, and reflect the stiffness to the uniaxial strains along these directions. The calculated value of C_{11} is 223.6/232.2 GPa at the PBE/GGA-D2 level. While for the orthorhombic black phosphorus, C_{22} is significantly larger than C_{11} and C_{33} due to its structural anisotropy[29], but it is smaller than the C_{11} elastic constant of K_4 phosphorus, indicating that the K_4 structure is stiffer than black phosphorus for strains along the *a*, *b*, and *c* axis. The benefit from the high stiffness is that the K_4 structure could avoid the sliding observed in the layered phosphorus structures under a shear stress. The resistance of sliding could make K_4 phosphorus more suitable for nano-mechanical applications. The single crystal bulk moduli of the phosphorus K_4 crystal and black phosphorus are calculated according to the formula of bulk modulus represented by single-crystal elastic constants[27]. The result for black phosphorus is in good agreement with the value estimated from fitting the energy-volume relationship[30].

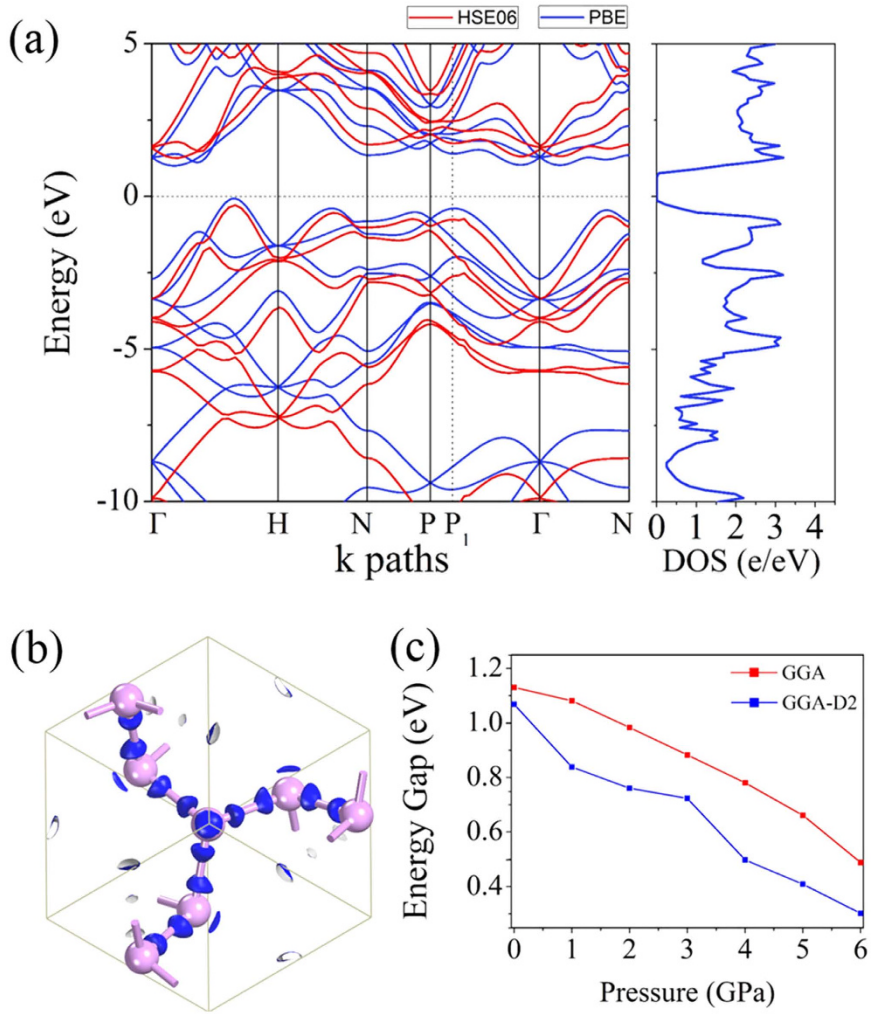

Figure 3. Electronic properties. (**a**) Electronic band structure and total DOS of K_4 phosphorus using the PBE (blue lines) and the HSE06 hybrid functionals (red lines). (**b**) Isosurces (0.76 e/Å^3) of the total valence electron density calculated using the PBE functionals. (**c**) Variation of band gap versus pressure calculated with the PBE and GGA-D2 functionals, respectively.

Electronic properties. We calculate the electronic band structure and corresponding total density of states (DOS) of K_4 phosphorus to study its electronic properties. The results are displayed in Fig. 3(a). At the PBE level, K_4 phosphorus is predicted to be an indirect band gap semiconductor with a band gap of 1.07 eV as the valence band maximum (VBM) and the conduction band minimum (CBM) lie at the different points along the Γ-H path. It is well-known that the PBE funtional underestimates the fundamental band gaps of semiconductors, thus the band gap of K_4 phosphorus is corrected by calculations using the more accurate HSE06 functional. As shown in Fig. 3(a). although both of the functionals give very similar band dispersions, the band gap of K_4 phosphorus calculated with HSE06 functional is increased to 1.54 eV. Figure 3(b) shows the isosurfaces of the toatal valence electron density of K_4 phosphorus. As mentioned above, the phosphorus atoms are sp^3 hybridized due to the three P-P covelent bonds and a lone electron pair, thus the valence electrons mainly distributed along the directions of the P-P bonds and the lone electron pair.

To investigate how the energy band gap of K_4 phosphorus changes with the applied hydrostatic pressure, we calculate the band gap as a function of the pressure, and plot the results in Fig. 3(c), which shows that the band gap of the K_4 phase decreases with volume compression under hydrostastic pressure. At the GGA level, the band gap decreases almost linealy from 1.13 eV to 0.49 eV as pressure increses from zero to 6 GPa. While at the GGA-D2 level, the band gap decreases from 1.07 eV to 0.30 eV within the same pressure range.

Optical properties. We next explore the potential applications of K_4 phosphorus in optoelectronics. The imaginary part of dielectric function of K_4 phosphorus, which is directly related to its optical absorbance, is calculated at the HSE06 level. For comparison, calculation for diamond silicon is also carried out by using the same approach. According to photon energy, the spectrum is divided into three parts, namely the infrared, visible, and ultraviolet regions, respectively. As shown in Fig. 4, the imaginary part of the dielectric function of K_4 phosphorus reaches the maximum at 3.18 eV, and follows by a minimum at 4.21 eV. According to the calculated results, K_4 phosphorus exhibits much stronger optical absorption than diamond silicon in the visible range. The absorption

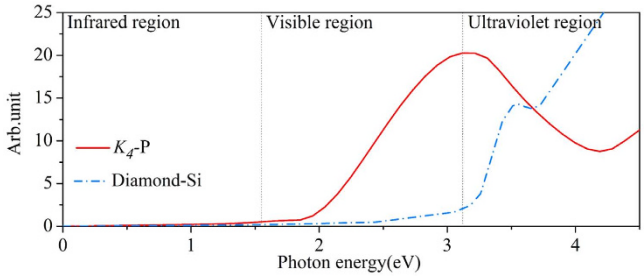

Figure 4. Optical absorption spectra. Imaginary part of dielectric function of K_4 phosphorus and diamond silicon calculated at the HSE06 level.

spectrum of K_4 phosphorus is also higher than that of diamond silicon from 3.12 to 3.66 eV in the near ultraviolet region. Currently, diamond silicon is still the leading material of solar cells[31]. It has an indirect band gap of 1.1 eV and a large direct gap of 3.3 eV, making it inefficient for sunlight absorption[32]. For K_4 phosphorus, although it is also an indirect band gap semiconductor, it possesses a direct band gap of 2.4 eV at P_1 point in the Brillouin zone (see Fig. 3(a)), which just lies in the middle part of the spectral range of visible light. As compared with diamond silicon, the smaller direct band gap of K_4 phosphorus makes it a better solar absorber. Based on above analysis, we conclude that K_4 phosphorus exhibits strong optical absorption in the visible and near ultraviolet region, making it a promising candidate for photovoltaics.

To provide a possible way to experimentally identify the K_4 phase of phosphorus from other phosphorus allotropes using Raman and infrared (IR) spectroscopy, we simulate the vibration properties of the K_4 structure at the Γ point. In order to verify the reliability of our calculations, we first perform the calculations for the *A*17 phase. From the analysis of the D_{2h} point group, the zone-center optical phonon modes of *A*17 can be classified into

$$\Gamma_{\text{optical}}(A17) = B_{1u}(I) + B_{2u}(I) + A_u + 2A_g(R) + B_{1g}(R) + B_{2g}(R) + 2B_{3g}(R),$$

where A_g, B_{1g}, B_{2g}, and B_{3g} are Raman-active modes (marked with "R"), B_{1u} and B_{2u} are infrared-active modes (marked with "I"), and the A_u mode is silent. The frequencies of the Raman-active modes calculated at GGA-D2 level are 185.2, 219.8, 347.6, 410.9, 426.2, and 454.1 cm^{-1}. These calculated results of Raman-active modes are in good agreement with earlier studies calculated using the same functional[29].

The phosphorus K_4 crystal belongs to T point group and possesses 4 irreducible representations, namely A, E, E^*, and T, respectively. The symmetries of its optical phonons at the zone center can be represented by the irreducible representations of T point group:

$$\Gamma_{\text{optical}}(K_4) = A(R) + E(R) + E^*(R) + 2T(I + R)$$

All the optical phonons are Raman active, and the T^1 and T^2 modes are also infrared active. The frequencies of the five Raman-active modes are 230.8 (T^1 mode), 311.3 (A mode), 392.1 (E mode), 392.1(E^* mode), and 403.9 (T^2 mode) cm^{-1}, respectively. The eigenvectors of the vibrational modes, as calculated at the GGA-D2 level, are illustrated in Fig. 5. These simulated Raman vibration results would be helpful to identify the K_4 phosphorus structure in experiment.

The satisfactory stability of K_4 phosphorus due to its ideal configuration of three-coordinated phosphorus atoms implies the possibility of the existence of this phase. Although it might be challenging to synthesize the K_4 crystal, there are some relevant experimental findings that are supportive of our predication. As mentioned above, the counterpart of K_4 phosphorus, the nitrogen K_4 crystal, was theoretically predicted *via* first principles calculations in 1992[33], and subsequently synthesized in 2004 through the polymerization of the molecular form of nitrogen at temperature above 2000 K and pressures above 110 GPa[18]. Similarly, the polymerization of the molecular form of phosphorus (tetrahedral P_4 molecules) was reported by Katayama *et al.*[34], where the transformation from molecular phosphorus to polymeric phosphorus occurred *via* thermal collision of the tetrahedral units of P_4 molecules, and then a 3D network of three-coordinated phosphorus was formed. During such process, the experimental conditions, such as elevated temperature and environment of the tetramers play a decisive role[35]. Therefore, we conclude that the phosphorus K_4 crystal could be synthesized through polymerization of molecular form of phosphorus at certain conditions as is the case with cg-N[18].

Summary

In summary, based on first principles calculations, we predict a 3D stable phosphorus K_4 phase. We show that the K_4 phosphorus structure is energetically metastable. The energy difference between the K_4 phase and black phosphorus is very small (0.04 eV/atom), similar to that between diamond and graphite. Compared to other stable phosphorus allotropes at ambient conditions, such as layered phosphorus structure (*A*17 and violet phosphorus) and the molecular forms of phosphorus (modifications of white phosphorus), K_4 phosphorus is a non-layered 3D phase with covalent bonds in all three dimensions. We demonstrate that K_4 phosphorus possesses special properties different from those of black phosphorus. K_4 phosphorus is stiffer than black phosphorus, and has a much larger band gap of 1.54 eV, which can be effectively tuned by appling hydrostastic pressure. K_4 phosphorus exhibits much better optical absorbance than diamond silicon from 1.50 to 3.66 eV, which may have potential applications in optoelectronics. In addition, all optical phonons of K_4 phosphorus at the first Brillouin zone center are

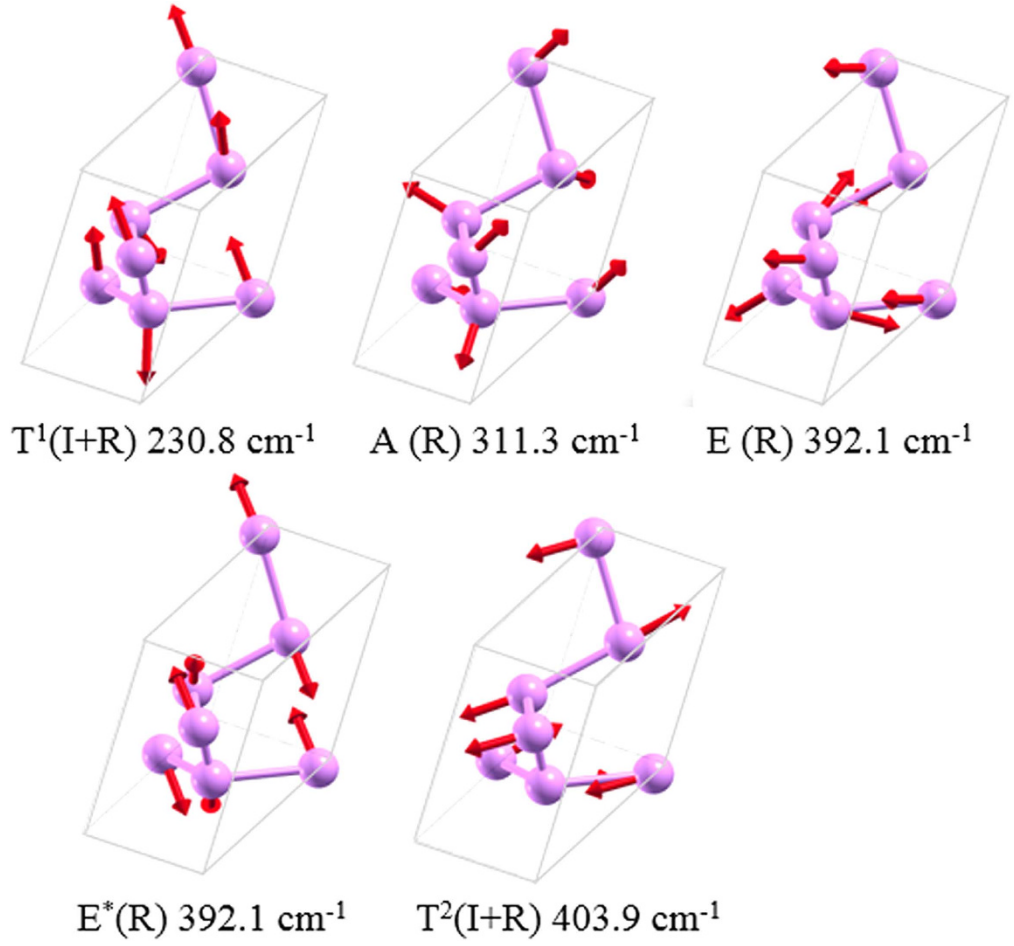

Figure 5. Vibrational modes. Snapshots of Raman-active and infrared-active modes for the K_4 phase of phosphorus in the primitive cell.

Raman active and the T^1 and T^2 modes are also infrared active, which can be used to identify this new allotrope of phosphorus experimentally in the furure. We hope that the present theoretical study would shed new lights on discovery of novel phosphorous materials and motivate experimental efforts in this direction.

Methods

First principles calculations are performed based on density functional theory (DFT) and the projector augmented wave (PAW) method[36] as implemented in the Vienna *Ab initio* Simulation Package (VASP)[37]. The electronic exchange-correlation interaction is incorporated in Perdew-Burke-Enzerhof (PBE) functional[38]. The plane-wave cutoff energy for wave function is set to 500 eV. Lattice parameters and atomic positions are allowed to fully relax within the conjugate gradient algorithm. Since van der Waals (vdW) interactions are important for phosphorus allotropes[12], the GGA-D2 functional[39] with long-range dispersion is used for the refinement of geometry in addition to the PBE functional. The Heyd-Scuseria-Ernzerhof (HSE06)[40] hybrid functional is then used for the high accuracy of electronic structure calculations. For structure optimization, the convergence thresholds are set at 10^{-4} eV and 10^{-3} eV/Å for total energy and force component, respectively. Monkhorst-Pack k-mesh[41] of $9 \times 9 \times 9$ is adopted to represent the first Brillouin zone. Thermal stability is studied using the Canonical ensemble (NVT) *ab initio* molecular dynamics (AIMD) simulations with temperature controlled by Nosé thermostat[42]. Phonon properties are calculated using the linear response method within density functional perturbation theory[25] as implemented in the Phonopy code[43]. Elastic constants are determined by the finite distortion formalism[27].

References

1. Kou, L., Chen, C. & Smith, S. C. Phosphorene: Fabrication, Properties, and Applications. *J. Phys. Chem. Lett.* **6,** 2794–2805 (2015).
2. Li, L. *et al.* Black phosphorus field-effect transistors. *Nat. Nanotechnol.* **9,** 372–377 (2014).
3. Liu, H. *et al.* Phosphorene: an unexplored 2D semiconductor with a high hole mobility. *ACS Nano* **8,** 4033–4041 (2014).
4. Bridgman, P. W. Two new modifications of phosphorus. *J. Am. Chem. Soc.* **36,** 1344–1363 (1914).
5. Wu, M., Fu, H., Zhou, L., Yao, K. & Zeng, X. C. Nine New Phosphorene Polymorphs with Non-Honeycomb Structures: A Much Extended Family. *Nano Lett.* **15,** 3557–3562 (2015).
6. Rodin, A., Carvalho, A. & Neto, A. C. Strain-induced gap modification in black phosphorus. *Phys. Rev. Lett.* **112,** 176801 (2014).
7. Jiang, J.-W. & Park, H. S. Negative poisson's ratio in single-layer black phosphorus. *Nat. Commun.* **5,** 4727 (2014).

8. Fei, R. *et al.* Enhanced thermoelectric efficiency via orthogonal electrical and thermal conductances in phosphorene. *Nano Lett.* **14,** 6393–6399 (2014).
9. Kou, L., Frauenheim, T. & Chen, C. Phosphorene as a Superior Gas Sensor: Selective Adsorption and Distinct I–V Response. *J. Phys. Chem. Lett.* **5,** 2675–2681 (2014).
10. Corbridge, D. E. C. *Structural chemistry of phosphorus*. (Elsevier Scientific Pub. Co., 1974).
11. Böcker, S. & Häser, M. Covalent structures of phosphorus: A comprehensive theoretical study. *Z. Anorg. Allg. Chem.* **621,** 258–286 (1995).
12. Bachhuber, F. *et al.* The Extended Stability Range of Phosphorus Allotropes. *Angew. Chem. Int. Ed.* **53,** 11629–11633 (2014).
13. Holleman, A. F. & Wiberg, E. *Lehrbuch der anorganischen Chemie*. (Walter de Gruyter, 1995).
14. Pfitzner, A., Bräu, M. F., Zweck, J., Brunklaus, G. & Eckert, H. Phosphorus Nanorods—Two Allotropic Modifications of a Long-Known Element. *Angew. Chem. Int. Ed.* **43,** 4228–4231 (2004).
15. Pfitzner, A. Phosphorus remains exciting! *Angew. Chem. Int. Ed.* **45,** 699–700 (2006).
16. Liu, J. *et al.* New Phosphorene Allotropes Containing Ridges with 2- and 4-Coordination. *J. Phys. Chem. C.* **119,** 24674–24680 (2015).
17. Sunada, T. CrystalsThatNatureMight MissCreating. *Notices of the AMS* **55** (2008).
18. Eremets, M. I., Gavriliuk, A. G., Trojan, I. A., Dzivenko, D. A. & Boehler, R. Single-bonded cubic form of nitrogen. *Nat. Mater.* **3,** 558–563 (2004).
19. Yaghi, O. M., Davis, C. E., Li, G. & Li, H. Selective Guest Binding by Tailored Channels in a 3-D Porous Zinc(II)–Benzenetricarboxylate Network. *J. Am. Chem. Soc.* **119,** 2861–2868 (1997).
20. Itoh, M. *et al.* New Metallic Carbon Crystal. *Phys. Rev. Lett.* **102,** 055703 (2009).
21. Yao, Y. *et al.* Comment on "New Metallic Carbon Crystal". *Phys. Rev. Lett.* **102,** 229601 (2009).
22. Dai, J., Li, Z. & Yang, J. Boron K_4 crystal: a stable chiral three-dimensional sp2 network. *Phys. Chem. Chem. Phys.* **12,** 12420–12422 (2010).
23. O'Keeffe, M., Peskov, M. A., Ramsden, S. J. & Yaghi, O. M. The reticular chemistry structure resource (RCSR) database of, and symbols for, crystal nets. *Accounts. Chem. Res.* **41,** 1782–1789 (2008).
24. Öhrström, L. & O'Keeffe, M. Network topology approach to new allotropes of the group 14 elements. *Z. Kristallogr.* **228,** 343–346 (2013).
25. Gonze, X. First-principles responses of solids to atomic displacements and homogeneous electric fields: Implementation of a conjugate-gradient algorithm. *Phys. Rev. B* **55,** 10337–10354 (1997).
26. Kaneta, C., Katayama-Yoshida, H. & Morita, A. Lattice Dynamics of Black Phosphorus. I. Valence Force Field Model. *J. Phys. Soc. Jpn.* **55,** 1213–1223 (1986).
27. Wu, Z.-j. *et al.* Crystal structures and elastic properties of superhard Ir N 2 and Ir N 3 from first principles. *Phys. Rev. B* **76,** 054115 (2007).
28. Cadelano, E. & Colombo, L. Effect of hydrogen coverage on the Young's modulus of graphene. *Phys. Rev. B* **85,** 245434 (2012).
29. Appalakondaiah, S., Vaitheeswaran, G., Lebegue, S., Christensen, N. E. & Svane, A. Effect of van der Waals interactions on the structural and elastic properties of black phosphorus. *Phys. Rev. B* **86,** 035105 (2012).
30. Zhang, S., Wang, Q., Chen, X. & Jena, P. Stable three-dimensional metallic carbon with interlocking hexagons. *Proc. Natl. Acad. Sci.* **110,** 18809–18813 (2013).
31. Jelle, B. P., Breivik, C. & Røkenes, H. D. Building integrated photovoltaic products: A state-of-the-art review and future research opportunities. *Sol. Energ. Mater. Sol. C.* **100,** 69–96 (2012).
32. Xiang, H., Huang, B., Kan, E., Wei, S.-H. & Gong, X. Towards direct-gap silicon phases by the inverse band structure design approach. *Phys. Rev. Lett.* **110,** 118702 (2013).
33. Mailhiot, C., Yang, L. & McMahan, A. Polymeric nitrogen. *Phys. Rev. B* **46,** 14419 (1992).
34. Katayama, Y. *et al.* A first-order liquid–liquid phase transition in phosphorus. *Nature* **403,** 170–173 (2000).
35. Hohl, D. & Jones, R. Polymerization in liquid phosphorus: Simulation of a phase transition. *Phys. Rev. B* **50,** 17047 (1994).
36. Blöchl, P. E. Projector augmented-wave method. *Phys. Rev. B* **50,** 17953 (1994).
37. Kresse, G. & Furthmüller, J. Efficient iterative schemes for ab initio total-energy calculations using a plane-wave basis set. *Phys. Rev. B* **54,** 11169 (1996).
38. Perdew, J. P., Burke, K. & Ernzerhof, M. Generalized Gradient Approximation Made Simple [Phys. Rev. Lett. 77, 3865 (1996)]. *Phys. Rev. Lett.* **78,** 1396–1396 (1997).
39. Osters, O. *et al.* Synthese und Identifizierung metastabiler Verbindungen: schwarzes Arsen – Fiktion oder Wirklichkeit? *Angewandte Chemie* **124,** 3049–3052 (2012).
40. Heyd, J., Scuseria, G. E. & Ernzerhof, M. Erratum:"Hybrid functionals based on a screened Coulomb potential"[J. Chem. Phys. 118, 8207 (2003)]. *J. Chem. Phys.* **124,** 219906 (2006).
41. Monkhorst, H. J. & Pack, J. D. Special points for Brillouin-zone integrations. *Phys. Rev. B* **13,** 5188 (1976).
42. Nosé, S. A unified formulation of the constant temperature molecular dynamics methods. *J. Chem. Phys.* **81,** 511–519 (1984).
43. Togo, A., Oba, F. & Tanaka, I. First-principles calculations of the ferroelastic transition between rutile-type and $CaCl_2$-type SiO_2 at high pressures. *Phys. Rev. B* **78,** 134106 (2008).

Acknowledgements

This work is partially supported by grants from the National Natural Science Foundation of China (NSFC-51471004), the National Grand Fundamental Research 973 Program of China (Grant No. 2012CB921404), and the Doctoral Program of Higher Education of China (20130001110033). The calculations were carried out at the National Supercomputer Center in Guangzhou, China.

Author Contributions

Q.W. designed the project; J.L. performed the calculations; J.L., S.Z., Y.G. and Q.W. analyzed the results and wrote the manuscript.

Additional Information

Supplementary information accompanies this paper at http://www.nature.com/srep

Competing financial interests: The authors declare no competing financial interests.

How to cite this article: Liu, J. *et al.* Phosphorus K_4 Crystal: A New Stable Allotrope. *Sci. Rep.* **6**, 37528; doi: 10.1038/srep37528 (2016).